Enhancing Pavement Surface Macrotexture Characterization by Using the Effective Area for Water Evacuation

Daniel E. Mogrovejo, Gerardo W. Flintsch, Samer W. Katicha, Edgar D. de León Izeppi, and Kevin K. McGhee

Adequate macrotexture characterization is an essential objective for transportation practitioners because primary pavement surface characteristics like friction, tire–pavement noise, splash and spray, and rolling resistance are significantly influenced by pavement macrotexture. This paper proposes an enhanced macrotexture characterization index based on the effective area for water evacuation (EAWE) that better estimates the potential of the pavement to drain water and provides improved correlations with two properties of pavement surfaces that are predominantly affected by macrotexture: friction and noise. A three-step methodology is proposed to compute the index: (*a*) a spike-removal procedure that assures the reliability of the texture profile data; (*b*) an enveloping profile calculation, which is necessary to delimit the area between the tire and the pavement when contact occurs; and (*c*) a definition of the EAWE, which serves as the index for characterizing macrotexture. Comparisons of current mean profile depth (MPD) and proposed EAWE macrotexture indexes by using 32 pavement sections confirmed that MPD overestimated the effective area for water evacuation between a tire and the pavement surface. Correlations for MPD and EAWE indexes with tire–pavement friction and noise were performed, and measurable improvements in correlations were achieved. Results show that it is possible to define a promising index on the basis of the EAWE that realizes advantages over MPD.

According to ISO Standard 13473-5:2009, pavement texture is the "deviation of a pavement surface from a true planar surface with a texture wavelength (λ) less than 0.5 m. Surface deviations of wavelengths greater than 0.5 m are known as unevenness or roughness" (*1*). The Permanent International Association of Road Congresses—World Road Association has established standard categories of texture (microtexture, macrotexture, megatexture) and roughness (unevenness), as well as the effects of texture and roughness on pavement surface properties (*2, 3*). This standard defines the range of the texture wavelength for macrotexture as greater than 0.5 mm and less than 50 mm. Macrotexture is likely the most influential texture category for most fundamental tire–pavement interactions (e.g., friction, tire–pavement noise, splash and spray, and rolling resistance).

In recent years the circular track (CT) meter, also known as a circular texture meter, and the mean profile depth (MPD) index have become widely accepted by practitioners for characterizing macrotexture. However, the CT meter is a static device that is not suitable for network-level measurements, while the MPD is an outdated method to characterize texture and can be improved.

With the objective of gathering more complete texture data and otherwise overcoming the limitations of the static test methods (e.g., amount of time required, highly localized results, and necessity for traffic control), dynamic methods (e.g., using high frequency laser equipment) have also been developed for texture measurements (*4–6*). With high-frequency laser equipment, significant resolution of texture measurements has been achieved even at highway speeds; however, two problems remain: (*a*) most of these methods still report MPDs and (*b*) standard procedures for dynamic methods are not yet available.

Recently, more realistic approaches for characterizing macrotexture have been explored. In these characterizations, there is a consideration of how the tire–pavement interaction results in enveloping profiles (representing the actual profile of the tire when it rolls over the pavement surface) that better take into account the effect on other pavement surface characteristics such as tire–pavement noise (*7*). A study conducted by Klein and Hamet proposed enveloping profiles for noise prediction on the basis of texture (*8*). Sandberg et al. proposed the use of enveloping to improve the modeling of rolling resistance (*9*).

On the basis of this research, the Virginia Tech Transportation Institute (VTTI) considered several of these models with the goal of applying the enveloping profile to macrotexture characterization rather than to texture–noise and texture–rolling resistance modeling. Three models were revised and evaluated: Clapp's envelopment procedure, which is based on a physical model that consists of evaluating the contact between a rigid body and a semi-infinite elastic body (*8*); the Klein–Hamet model, which is based on calculation of vertical displacement of the border of an elastic medium under

D. E. Mogrovejo, Faculty of Engineering, Department of Civil Engineering, University of Cuenca, Avenida 12 de Abril and Agustin Cueva, Cuenca, Ecuador. G. W. Flintsch, Charles E. Via, Jr., Department of Civil and Environmental Engineering, and S. W. Katicha and E. D. de León Izeppi, Center for Sustainable Transportation Infrastructure, Virginia Tech Transportation Institute, Virginia Polytechnic Institute and State University, 3500 Transportation Research Plaza, Blacksburg, VA 24061. K. K. McGhee, Virginia Center for Transportation Innovation and Research, 530 Edgemont Road, Charlottesville, VA 22903. Corresponding author: D. E. Mogrovejo, daniel.mogrovejo@ucuenca.edu.ec.

Transportation Research Record: Journal of the Transportation Research Board, No. 2591, Transportation Research Board, Washington, D.C., 2016, pp. 80–93.
DOI: 10.3141/2591-10

the influence of a vertical force (*8,* J. Hamet, P. Klein, F. Anfosso, D. Duhamel, A. Fadavi, and B. Begue, unpublished work, 2002); and the von Meier model, which is based on a mathematical–mechanistic approach that uses the mathematical limitation of the second-order derivative of the discretized texture sample (*8–10*). This last model resulted in the best fit for the purpose of macrotexture characterization because of its versatility and customizable settings (as detailed in the methodology section of this paper).

PROBLEM STATEMENT

The CT meter and other static methods for characterizing texture (e.g., the volumetric test method, ASTM E965) do not lend themselves to comprehensive or network-level testing. Moreover, significant variations in the eight CT meter sectors have been found (R. M. Perera, M. R. Orthmeyer, E. de León Izeppi, unpublished work, 2013). These shortcomings could be addressed with dynamic methods that also report the MPD (ASTM E1845), such as the VTTI method (*4*). However, by definition the MPD is calculated by using the peaks in a high-resolution profile, and thus the resulting index may not represent the actual potential of the pavement to drain water, which may be the most desired safety feature of the pavement. Furthermore, although macrotexture is known to greatly influence important surface functions, strong correlations of MPD with these functional characteristics are not well defined.

All of these problems justify the need for a better approach to macrotexture characterization. Thus, the use of an improved (multiple representation) index is proposed in this paper.

OBJECTIVE

The objective of this study was to propose an enhanced macrotexture characterization index that provides stronger correlations with pavement surface properties affected by macrotexture (tire–pavement friction and noise) by using an estimate of the effective area for water evacuation (EAWE).

APPROACH

Sites

Thirty-two road sections were selected for this study; they cover most of the asphalt types used in Virginia, including dense-, gap-, and open-graded mixes, as well as combinations of aggregate sizes, binders, and rubber modification.

Twelve of the 32 sections were selected from the Virginia Smart Road, a 2.2-mi, controlled-access test track, located at the Virginia Smart Road in Blacksburg, Virginia (*11*). Figure 1 shows an aerial view of the Virginia Smart Road, with pictures of the sections chosen and their details.

The remaining 20 of the 32 sections were chosen from three demonstration projects of the Virginia Quiet Pavement Implementation Program (VQPIP). These projects are located on State Route 199, west of Williamsburg; on State Route 286 in Fairfax County; and on State Route 288 near Chester (*12*). Figure 2 shows the diagrams for these projects and the sections, as well as the pictures of the corresponding pavement type and details about the pavement.

Equipment

Measurements for macrotexture, friction, and noise were performed for this study with the assumption that friction and noise are primary pavement surface characteristics that are influenced by macrotexture.

For texture measurements, two different sets of data were collected: (*a*) static measurements, with the CT meter, and (*b*) dynamic measurements, with a high-speed laser device (HSLD) that provided the data to be used for deriving both the MPD and the proposed index based on the EAWE.

For testing on the Virginia Smart Road, two CT meter devices (Figure 3*a*) were used for repeatability purposes. The measurements were made and the analysis was performed in accordance with ASTM E2157. Before the static measurements, precalibration that included checking for the proper functioning by using a calibration plate was performed for both devices with successful results. For the VQPIP sections, one CT meter was used. One HSLD (Figure 3*b*) capable of collecting measurements at different speeds [between 25 and 65 mph (40 and 105 km/h)] was also used to gather the dynamic measurements on all sites (Virginia Smart Road and VQPIP sections). This HSLD uses a laser spot with a diameter of 0.2 mm and a sampling frequency of 64 kHz (*4, 5*); more detailed information about this device can be found in the user's manual for the Selcom optocator (*13*).

A GripTester was used for friction measurements (Figure 3*c*). The GripTester, which conforms to ASTM E2340, operates at a constant slip of 16%.

Tire–pavement noise was measured according to AASHTO TP 76-12. VTTI's on-board sound intensity (OBSI) equipment (shown in Figure 3*d*) was used for all sites (*14*).

Data Collection in the Field

The following measurements were made with the CT meter, HSLD, GripTester, and OBSI device:

- CT meter. At least 10 measurements with each CT meter were performed for each section on the Virginia Smart Road (which means at least 20 CT meter measurements were available for each section for the calculation of an average MPD). For the VQPIP sections, traffic control was necessary because these are state routes with annual average daily traffic counts between 23,000 and 41,000. At least five measurements were performed for each section [e.g., stone matrix asphalt (SMA) 9.5], in each direction (e.g., northbound and southbound), and for each location [e.g., State Route (SR-199)]. Fewer measurements was collected on the VQPIP sections because these sections are open to traffic (unlike the Virginia Smart Road sections, which are on a closed facility). All CT meter measurements (that is, from all eight of the CT meter's sectors) were included in the results to more accurately account for variability of the macrotexture.
- HSLD. Ten runs at 50 mph (80.5 km/h) were performed on the Virginia Smart Road sections and three runs (at the same speed) for the VQPIP sections (resulting in a total of 180 runs for analysis). Raw data were collected at a frequency of 64 kHz and analyzed every 0.5 mm. A despiking procedure was performed over every raw data set before the MPD was calculated and the enveloping profile to be used for the EAWE-based index (explained below) was determined.
- GripTester. Twelve repeat GripTester runs were made over the Virginia Smart Road sections and three were performed at each VQPIP project. Testing was performed at 40 mph and data collected every 3 ft along the entire length of every section.

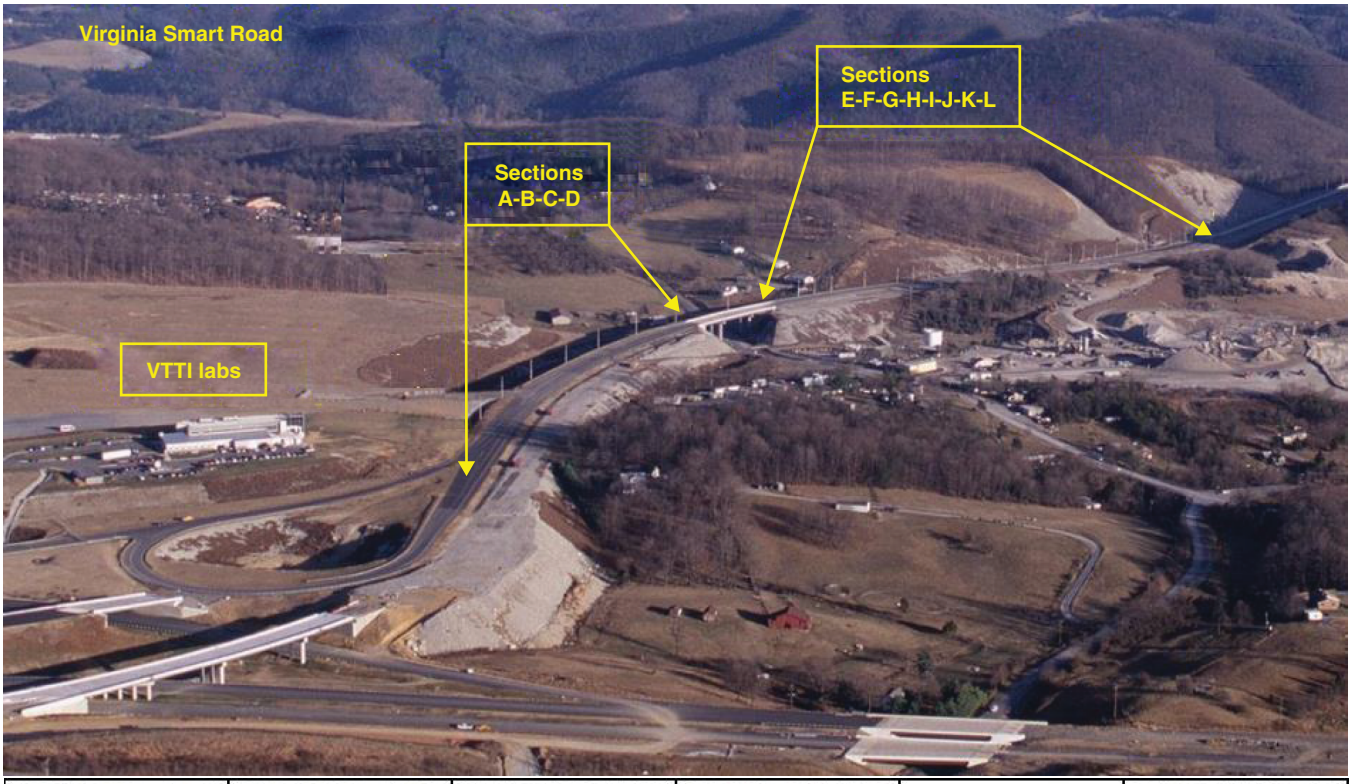

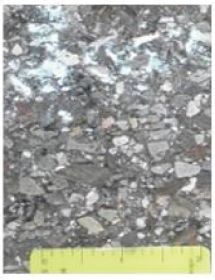				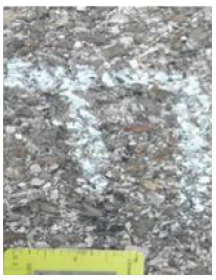	
A–SMA-12.5D PG 70-22 Section Length: 106 m (347 ft)	B–SM-9.5D PG 70-22 Section Length: 88 m (289 ft)	C–SM-9.5E PG 76-22 Section Length: 89 m (292 ft)	D–SM-9.5A PG 64-22 Section Length: 124 m (407 ft)	E–SM-9.5D PG 70-22 Section Length: 82 m (268 ft)	F–SM-9.5D PG 70-22 Section Length: 92 m (302 ft)
				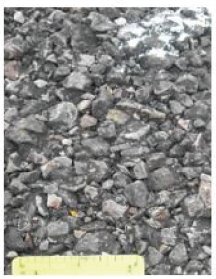	
G–SM-9.5D PG 70-22 Section Length: 93 m (304 ft)	H–SM-9.5D PG 70-22 Section Length: 89 m (292 ft)	I–SM-9.5A PG 64-22 Section Length: 103 m (338 ft)	J–SM-9.5D PG 70-22 Section Length: 85 m (280 ft)	K–OGFC PG 76-22 Section Length: 92 m (302 ft)	L–SMA-12.5D PG 70-22 Section Length: 99 m (326 ft)

FIGURE 1 Virginia Smart Road test sections (SM = stone matrix; OGFC = open-graded friction course).

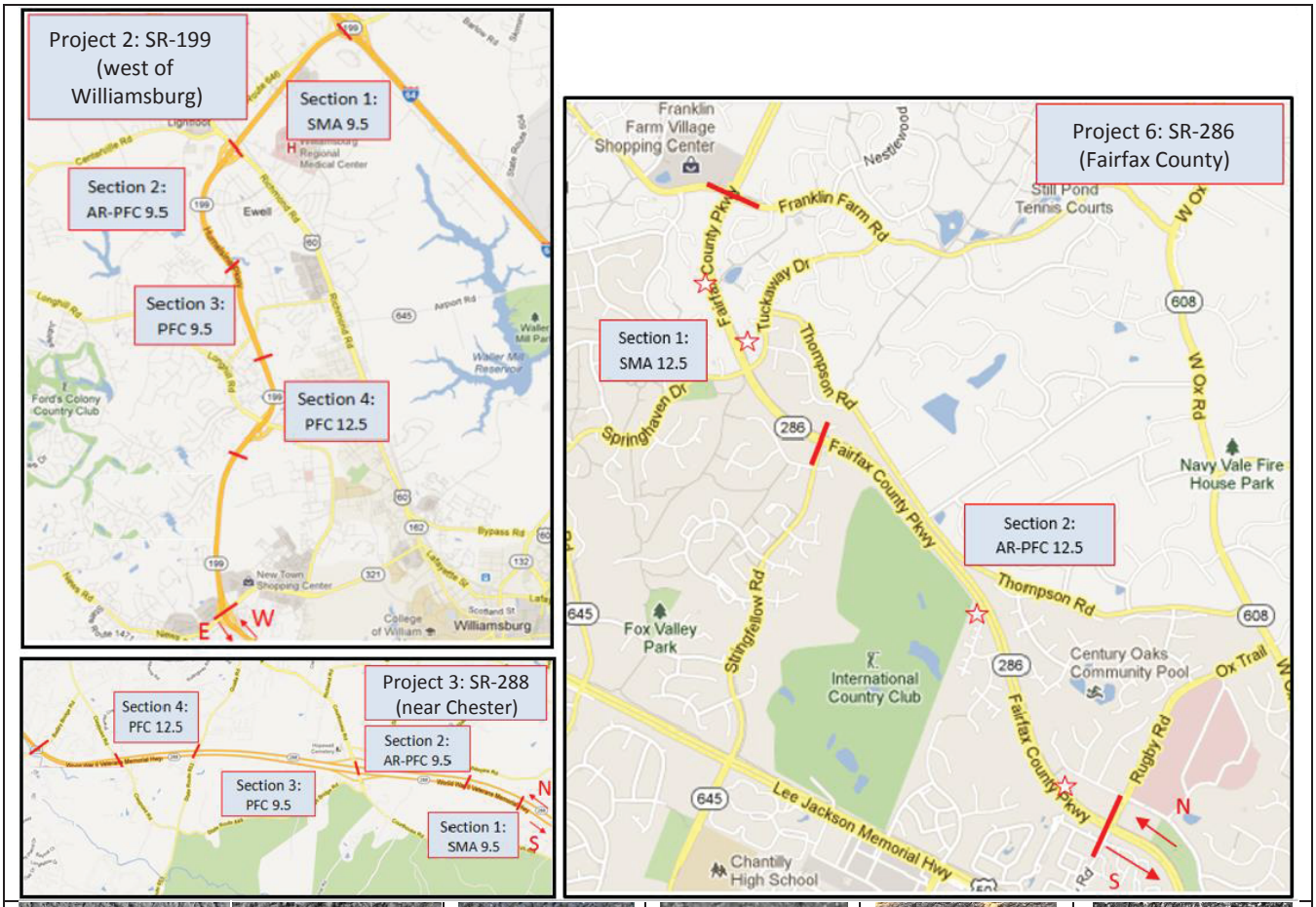

SMA 9.5 Stone matrix asphalt pavement, PG 76-22, 1.5 in. thick, maximum aggregate size: 9.5 mm, 165 lb/yd^2	AR-PFC 9.5 Asphalt rubber–porous friction course, 1 in. thick, maximum aggregate size: 9.5 mm, 90 lb/yd^2	PFC 9.5 Porous friction course, PG 70-28, 1 in. thick, maximum aggregate size: 9.5 mm, 90 lb/yd^2	PFC 12.5 Porous friction course, PG 70-28, 1.5 in. thick, maximum aggregate size: 12.5 mm 180 lb/yd^2 in SR-199, 135 lb/yd^2 in SR-288	SMA 12.5 Stone matrix asphalt pavement, PG 76-22, maximum aggregate size: 12.5 mm	AR-PFC 12.5 Asphalt rubber–porous friction course, maximum aggregate size: 12.5 mm
Section names:					
SR-199 SMA 9.5 E SR-199 SMA 9.5 W SR-288 SMA 9.5 N SR-288 SMA 9.5 S	SR-199 AR-PFC 9.5 E SR-199 AR-PFC 9.5 W SR-288 AR-PFC 9.5 N SR-288 AR-PFC 9.5 S	SR-199 PFC 9.5 E SR-199 PFC 9.5 W SR-288 PFC 9.5 N SR-288 PFC 9.5 S	SR-199 PFC 12.5 E SR-199 PFC 12.5 W SR-288 PFC 12.5 N SR-288 PFC 12.5 S	SR-286 SMA 12.5 N SR-286 SMA 12.5 S	SR-286 AR-PFC 12.5 N SR-286 AR-PFC 12.5 S

FIGURE 2 VQPIP test sections.

(a)

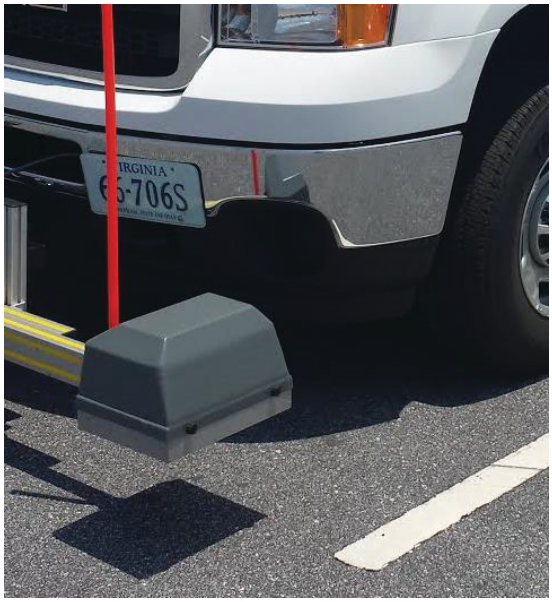

(b)

(c)

(d)

FIGURE 3 Test equipment used for study: (*a*) CT meter for static macrotexture measurements (MPD) (*4*), (*b*) HSLD for dynamic macrotexture measurements (*4*), (*c*) GripTester for slip friction measurements, and (*d*) OBSI for tire–pavement noise measurements (*14*).

• OBSI. Tire–pavement noise measurements on the Virginia Smart Road were made as follows: two valid runs for Section K (minimum number of valid runs according to AASHTO TP 76-12), three valid runs over Sections L and A, five valid runs over Section B, and seven valid runs over Sections E, F, G, and H. For the VQPIP sections, at least three valid runs were performed for each section. A run was considered valid if it met these four criteria stated in the standard: coherence pressure-intensity index, direction of the sound intensity vector, and standard deviation. Detailed information about this validation can be found in Mogrovejo et al. (*12*).

Calculating the Proposed Index by Using the EAWE

An improved pavement surface texture index, the EAWE index (in mm^2), is proposed in this paper. Three crucial steps structure the proposed methodology for computing the index:

1. Mandatory spike-removal process applied to the raw HSLD data;
2. Calculation of the enveloping profile, which is the profile that the tire creates when in contact with the surface of the pavement; and
3. Calculation of the corresponding effective depth for water evacuation (EDWE) from which the EAWE index is derived.

Step 1. Spike Removal from HSLD Measurements

It is widely known that all HSLD measurements have "noise" in the data in the form of spikes that must be removed before analysis takes place (*4, 5, 15*). In this study, the proposed indexes were correctly calculated for macrotexture characterization by applying a spike-removal method developed by the authors [Katicha et al. (*4*)] to the raw data that had been gathered.

The spike-removal method is a two-step algorithm. First, the algorithm determines the distribution of texture measurements (after high-pass filtering of the raw data for slope removal) by using the family of generalized Gaussian distributions; this step allows for the tail of the distribution to be heavier or thinner than the normal distribution. Second, the algorithm uses the false discovery rate method to control the proportion of wrongly identified spikes out of all identified spikes. The false discovery rate control allows for an adaptive threshold selection that differentiates between valid measurements and spikes.

Step 2. Calculation of the Enveloping Profile

The envelopment procedure developed by von Meier et al. was chosen because a mathematical–empirical model allows for the adjustment of the resulting enveloping profile according to tire stiffness (a required feature for comparison of the EAWE and MPD as explained and depicted in the results that follow). This procedure limits (or reduces) the second-order derivative of the profile to a given limit value (d^*), which is a measure of the elasticity of the tire rubber expressed in mm/mm^2 or mm^{-1}). Von Meier et al. determined empirical values for d^* from measurements of the deformation of a tire pressed onto various idealized profiles made of steel rods with different diameters and spacing; in their work, enveloping profiles with d^* values of 0.1, 0.054, and 0.027 were presented (*10*).

A revised version of the model by von Meier et al. [including "form" corrections made by Goubert (*7*) and restructuring by VTTI for fitting with MATLAB codification] was used for the calculations of the enveloping profile. The corrected and restructured model is diagrammed in Figure 4.

Step 3. Effective Area and Effective Depth for Evacuation of Water or Air or Both

The proposed EAWE index (in mm^2), represents the area between the resulting tire enveloping profile and the actual pavement texture profile when tire–pavement contact occurs.

The EAWE (in mm^2) can be reported in three ways:

1. As a vector of values ($\widehat{\text{EAWE}}$), which means one value for every data point in the profile. This vector is arranged as follows:

$$\widehat{\text{EAWE}} = [\text{EAWE}_1, \text{EAWE}_2, \ldots, \text{EAWE}_i, \ldots, \text{EAWE}_n] \quad (1)$$

where n is the number of data points in the texture profile and

$$\text{EAWE}_i = \left(\frac{b_i + b_{i+1}}{2} * h \right) \quad (2)$$

where b_i results from subtracting the ith data point in the original pavement profile from the ith data point in the enveloping profile and $h = 0.5$ mm, the spacing between data points in the profiles.

2. As a vector of accumulated values with a base length of 100 mm ($\widehat{\text{EAWE}}_{100}$), which means one value for every 100 mm (every 200 data points) in the profile. The 100-mm base length was chosen to be consistent with then MPD base length when analyzed with the HSLD, and thus allow point-by-point comparison of the two indexes. This vector is arranged as shown in the following equation [where $m = f(n)$]:

$$\widehat{\text{EAWE}}_{100} = [\text{EAWE}_{100_1}, \text{EAWE}_{100_2}, \ldots, \text{EAWE}_{100_m}] \quad (3)$$

where

$$\text{EAWE}_{100_1} = \sum_{j=1}^{200} \text{EAWE}_j, \text{EAWE}_{100_2} = \sum_{j=201}^{400} \text{EAWE}_j, \ldots, \text{EAWE}_{100_m} = \sum_{j=n-199}^{n} \text{EAWE}_j \quad (4)$$

where j is the auxiliary variable.

3. As a scalar value (EAWE), which means a single average value with a 100-mm baseline that represents the whole section, calculated as follows:

$$\text{EAWE} = \frac{\sum_{j=1}^{m} \text{EAWE}_{100_j}}{m} \quad (5)$$

Finally, the corresponding EDWE (in mm) is defined and can be reported as a scalar value (EDWE), which means a single average value with a 100-mm baseline that represents the whole section, calculated as follows:

$$\text{EDWE} = \frac{\text{EAWE}}{100} \quad (6)$$

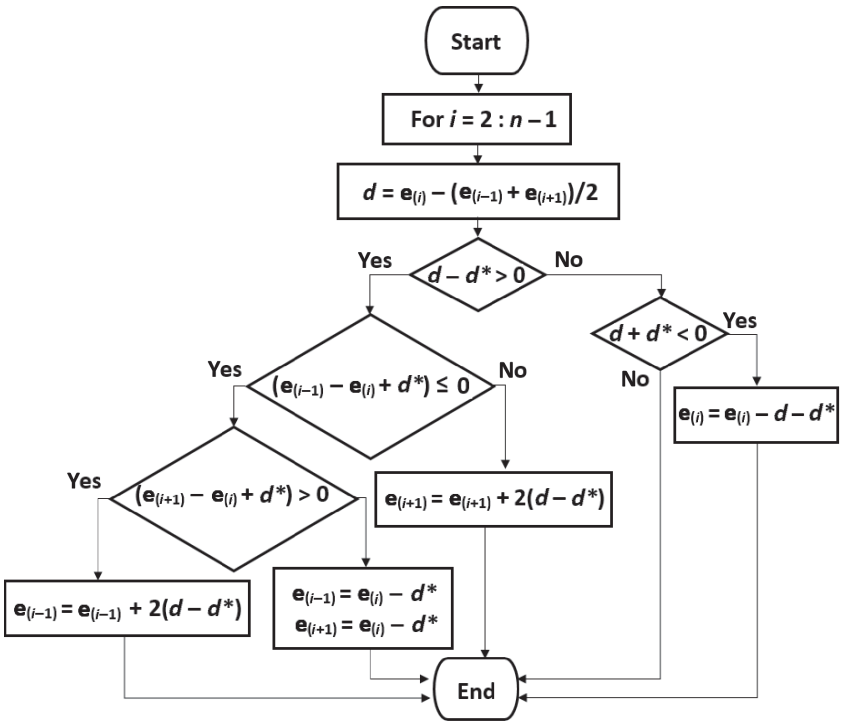

where

n = number of data points from the original pavement texture profile obtained with the HSLD;
d^* = given maximum value (e.g., d^* = 0.054 mm/mm^2) representing the elasticity of the tire rubber;
d = changing aid variable; and
e = resulting enveloping profile (vector).

FIGURE 4 Diagram for enveloping profile calculation.

The vector representations of the EAWE allow every location in the section to be analyzed [for example, to find significant variation of texture, section changes, and critical spots (relatively low EAWE)].

RESULTS

Step 1. Spike Removal

Spike removal was performed for all HSLD raw data. Figure 5 is a snapshot of the beginning of a randomly selected section, showing the original measurements and the measurements after spike removal.

Step 2. Calculation of Enveloping Profile

For the chosen enveloping profile method, d^* is defined as a measure for the elasticity of the tire rubber. Different values for d^* (0.054, 0.027, and 0.01) in mm/mm^2 were obtained by von Meier et al. during their empirical experimentation with different artificial surfaces (containing peaks and valleys with different amplitudes and longitudes) (*10*).

The larger the value of d^*, the more the enveloped profile will follow the original pavement profile, meaning that high d^* values represent soft rubber tires and low d^* values represent stiff tires. For this study, very small values for d^* (e.g., 0.001, representing significantly stiffer rubber tires) are used in addition to the d^* values used by von Meier et al. (*10*) to test the hypothesis of overestimation of the EAWE when the MPD is used (indicated in Step 3).

Therefore, the analysis of the enveloping profile was performed for all 180 denoised profiles with four different d^* values (0.054, 0.027, 0.01, 0.001), which can be related to medium soft, medium hard, stiff, and very stiff tires, respectively. Because the focus of this paper is pavement macrotexture, rather than the geometric properties of the tire, a smooth tire is assumed here.

Examples of the resulting enveloping profiles, for different tire stiffnesses, are presented in Figures 6 and 7, which show the results for a gap- and open-graded mix, respectively. As expected, the higher the tire stiffness (represented by the smaller d^* values), the higher the EAWE.

Step 3. Calculation of the EAWE and the EDWE

Because the MPD is calculated as the average of the peak levels on each half of the baseline profile minus the average level (which means using the peaks, by definition), then the MPD is believed to overestimate the pavement's EAWE.

To that point, Figure 8 illustrates how the MPD overestimated the ability of the pavement to evacuate water, because these mean depths (function of the peaks) are higher in magnitude than the average

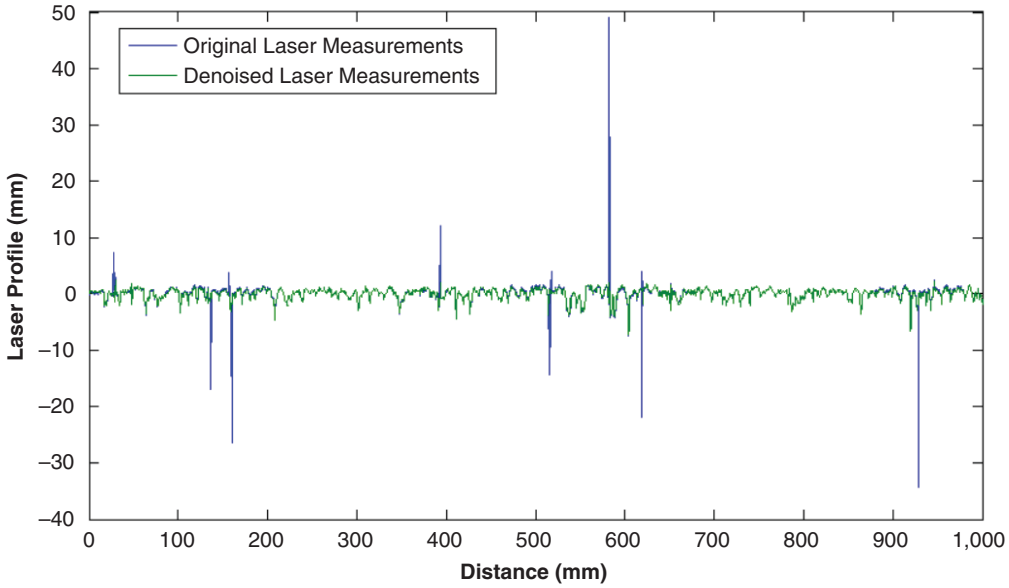

FIGURE 5 HSLD measurements, with and without spikes (first meter of Section SR-199 AR-PFC 9.5 E).

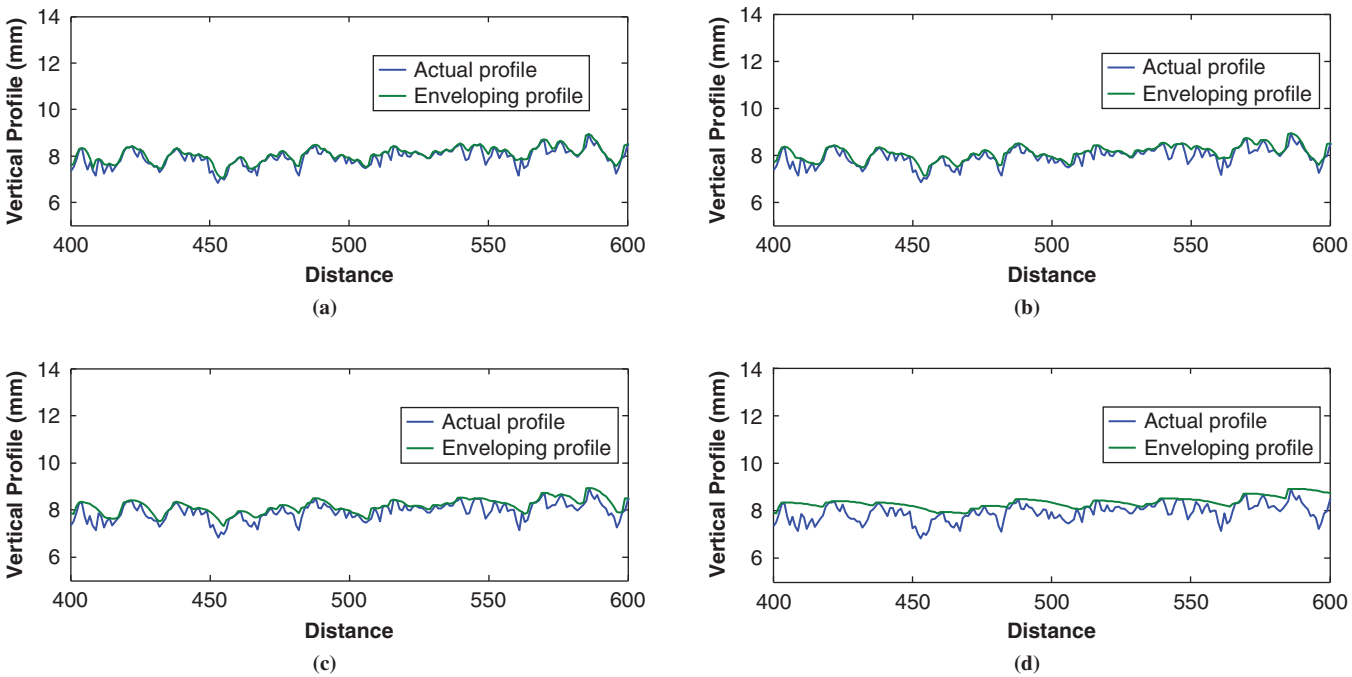

FIGURE 6 Illustration of enveloping profile calculated for different tire stiffnesses for a gap-graded asphalt mix (for 100 mm of Section SR-288 SMA 9.5 N, with data points every 0.5 mm): (*a*) $d^* = 0.054$, (*b*) $d^* = 0.027$, (*c*) $d^* = 0.010$, and (*d*) $d^* = 0.001$.

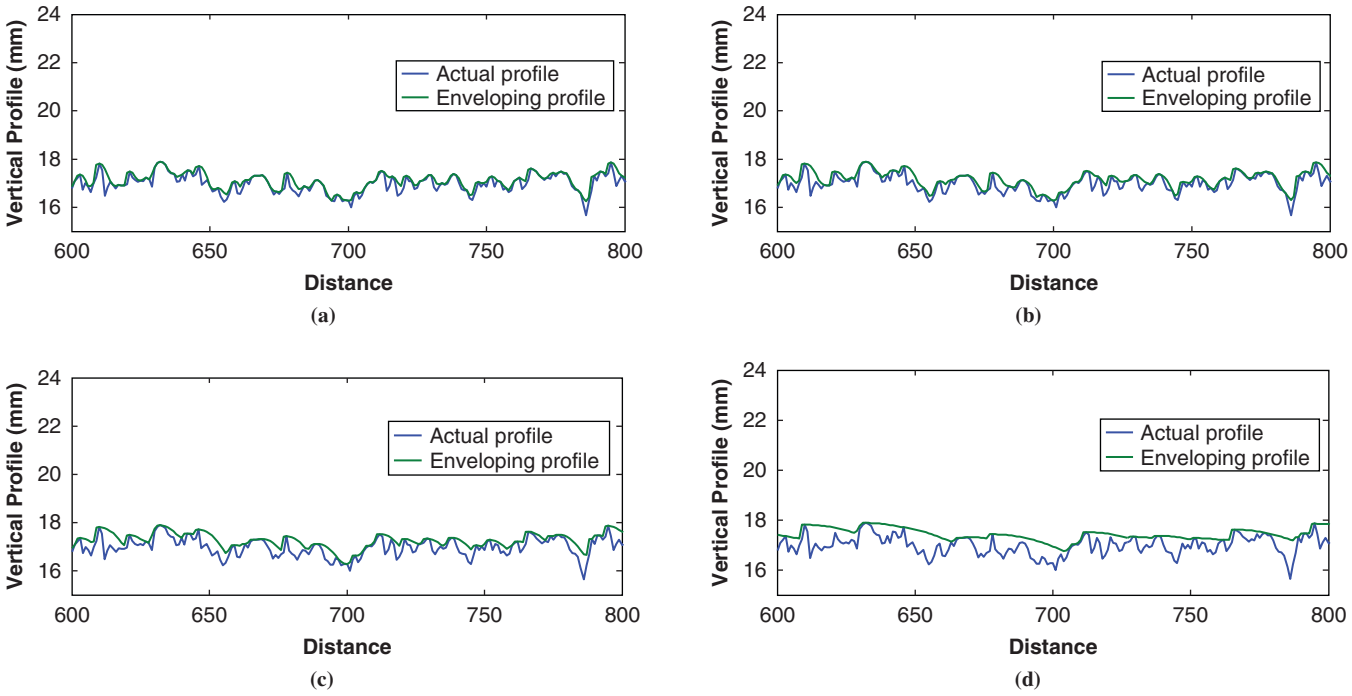

FIGURE 7 Illustration of enveloping profile calculated for different tire stiffnesses for a porous asphalt mix (for 100 mm of Section K–OGFC, with data points every 0.5 mm): (*a*) $d^* = 0.054$, (*b*) $d^* = 0.027$, (*c*) $d^* = 0.010$, and (*d*) $d^* = 0.001$.

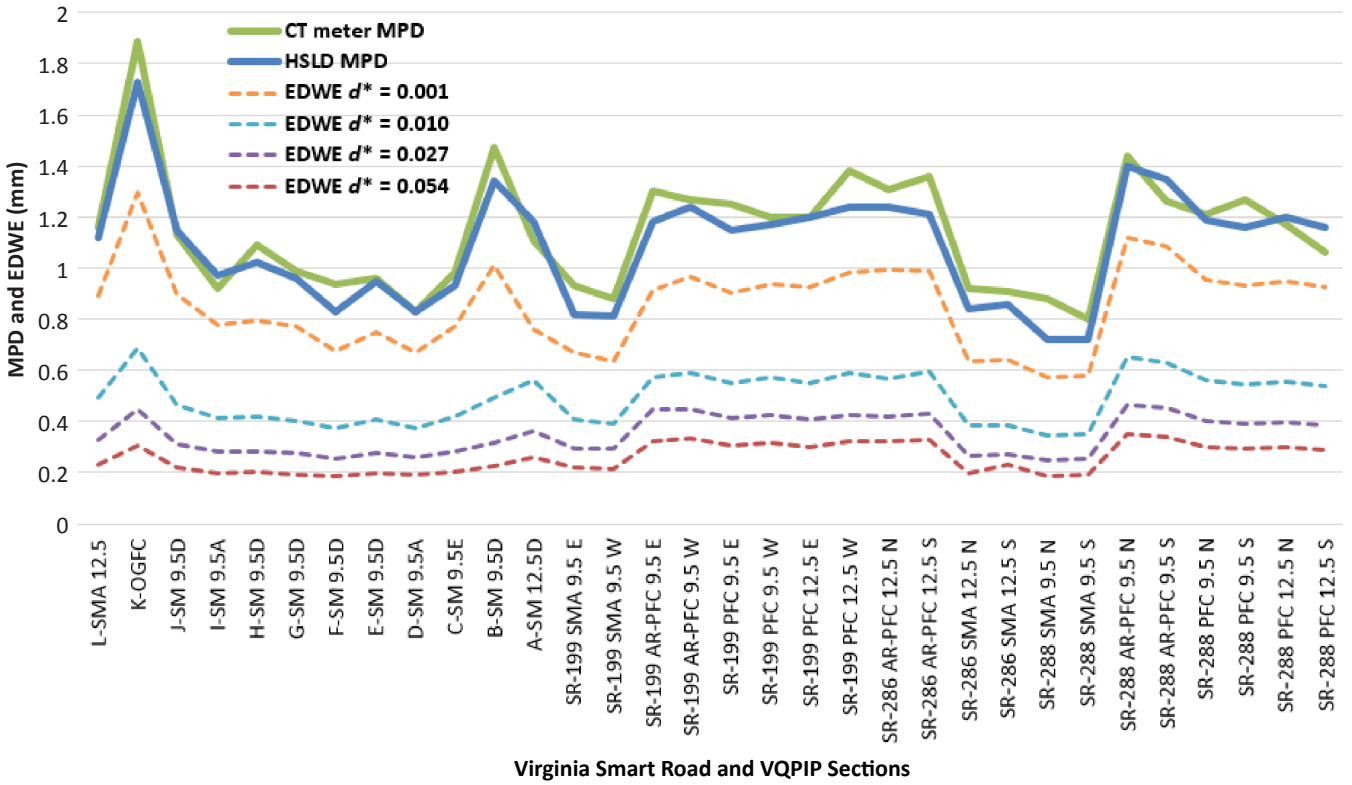

FIGURE 8 Comparison of macrotexture characterization indexes.

effective depth of the resulting area between the tire and the pavement as represented by the EDWE.

A sensitivity analysis (varying tire stiffness) confirms that the MPD models the area similarly to the way the EAWE does only when relatively little tire rubber deformation is allowed, which is not what really happens. That is, the EDWE index tends to resemble the MPD in magnitude only when a relatively small d^* value of 0.001 is used (theoretically representing a significantly stiff tire).

Furthermore, correlations with friction and tire–pavement noise, which are two pavement surface characteristics that are heavily influenced by macrotexture (*2, 3*), also improve when the EAWE is used instead of the MPD for all tire stiffnesses. These improved correlations hold, regardless of the system from which the raw data originated (CT meter or HSLD).

Table 1 summarizes a substantial data set of macrotexture, friction (measured by the GripTester), and tire–pavement noise (OBSI) data. It represents 340 CT meter runs for texture (for the MPD), 180 HSLD runs for texture (for the MPD), 720 HSLD runs for texture (for the EAWE), 204 GripTester runs for friction (expressed by the grip number), and 101 OBSI runs for noise (expressed by the intensity level).

The practical use of texture characterization is to explain how other pavement characteristics, such as friction and noise, are affected by texture. Figures 9 and 10 show that the EAWE, being a

TABLE 1 Summary of Texture, Friction, and Noise Indexes

	Macrotexture											
	MPD (mm)		EAWE (mm)				EDWE (mm)					
Section	CT Meter	HSLD	0.054	0.027	0.010	0.001	0.054	0.027	0.010	0.001	Friction[a]	Noise[b] [dB(A)]
L-SMA 12.5	1.16	1.12	23.29	33.09	49.14	89.33	0.23	0.33	0.49	0.89	0.53	101.1
K-OGFC	1.89	1.73	30.54	44.56	68.43	129.49	0.31	0.45	0.68	1.29		99.7
J-SM 9.5D	1.13	1.15	21.92	31.30	46.52	89.85	0.22	0.31	0.47	0.90	0.57	
I-SM 9.5A	0.92	0.97	19.72	28.14	41.34	77.78	0.20	0.28	0.41	0.78	0.66	
H-SM 9.5D	1.09	1.02	20.00	28.34	41.75	79.58	0.20	0.28	0.42	0.80		102.3
G-SM 9.5D	0.99	0.96	19.15	27.44	40.40	77.07	0.19	0.27	0.40	0.77		102.3
F-SM 9.5D	0.94	0.83	18.42	25.65	37.10	67.40	0.18	0.26	0.37	0.67		102.3
E-SM 9.5D	0.96	0.95	19.72	27.86	40.73	74.95	0.20	0.28	0.41	0.75		102.3
D-SM 9.5A	0.83	0.83	18.98	26.09	37.59	66.83	0.19	0.26	0.38	0.67	0.52	
C-SM 9.5E	0.98	0.93	20.47	28.41	42.00	77.35	0.20	0.28	0.42	0.77	0.56	
B-SM 9.5D	1.47	1.34	22.53	31.80	49.59	100.88	0.23	0.32	0.50	1.01	0.67	101.1
A-SM 12.5D	1.11	1.18	25.89	36.32	56.38	75.82	0.26	0.36	0.56	0.76	0.61	100.7
SR-199 SMA 9.5 E	0.93	0.82	21.85	29.43	40.62	67.25	0.22	0.29	0.41	0.67	0.65	102
SR-199 SMA 9.5 W	0.88	0.81	21.30	29.18	39.33	63.62	0.21	0.29	0.39	0.64	0.64	102.2
SR-199 AR-PFC 9.5 E	1.3	1.18	32.06	44.75	57.38	91.31	0.32	0.45	0.57	0.91	0.72	99.2
SR-199 AR-PFC 9.5 W	1.27	1.24	33.34	44.87	58.89	96.59	0.33	0.45	0.59	0.97		99.3
SR-199 PFC 9.5 E	1.25	1.15	30.56	41.60	55.08	90.43	0.31	0.42	0.55	0.90	0.73	
SR-199 PFC 9.5 W	1.2	1.17	31.58	42.56	57.41	94.00	0.32	0.43	0.57	0.94	0.68	100.1
SR-199 PFC 12.5 E	1.2	1.2	30.20	40.72	54.97	92.36	0.30	0.41	0.55	0.92	0.67	
SR-199 PFC 12.5 W	1.38	1.24	32.08	42.51	58.84	98.31	0.32	0.43	0.59	0.98	0.68	100.9
SR-286 AR-PFC 12.5 N	1.31	1.24	31.98	42.06	56.74	99.33	0.32	0.42	0.57	0.99		98.7
SR-286 AR-PFC 12.5 S	1.36	1.21	32.94	43.18	59.54	98.90	0.33	0.43	0.60	0.99	0.68	97.5
SR-286 SMA 12.5 N	0.92	0.84	19.68	26.51	38.66	63.32	0.20	0.27	0.39	0.63	0.67	103.1
SR-286 SMA 12.5 S	0.91	0.86	23.06	26.91	38.77	64.28	0.23	0.27	0.39	0.64	0.62	103.2
SR-288 SMA 9.5 N	0.88	0.72	18.60	24.89	34.32	57.51	0.19	0.25	0.34	0.58	0.66	103.3
SR-288 SMA 9.5 S	0.8	0.72	18.89	25.30	34.94	58.09	0.19	0.25	0.35	0.58	0.60	103
SR-288 AR-PFC 9.5 N	1.44	1.4	35.10	46.46	65.28	111.98	0.35	0.46	0.65	1.12	0.67	100.9
SR-288 AR-PFC 9.5 S	1.26	1.35	33.88	45.22	63.21	108.40	0.34	0.45	0.63	1.08	0.70	101.2
SR-288 PFC 9.5 N	1.21	1.19	30.17	40.10	56.14	95.18	0.30	0.40	0.56	0.95	0.69	101.7
SR-288 PFC 9.5 S	1.27	1.16	29.35	39.00	54.60	93.03	0.29	0.39	0.55	0.93	0.67	102.2
SR-288 PFC 12.5 N	1.17	1.2	30.06	39.86	55.65	94.84	0.30	0.40	0.56	0.95	0.70	101.2
SR-288 PFC 12.5 S	1.06	1.16	28.98	38.53	53.96	92.65	0.29	0.39	0.54	0.93	0.64	100.6

NOTE: Sections A through L are listed in reverse alphabetical order because that is the order of testing on the Smart Road. Blank cells = data not collected; E = eastbound; W = westbound; N = northbound; S = southbound.
[a]Friction expressed as grip number (GN).
[b]Noise expressed as intensity level.

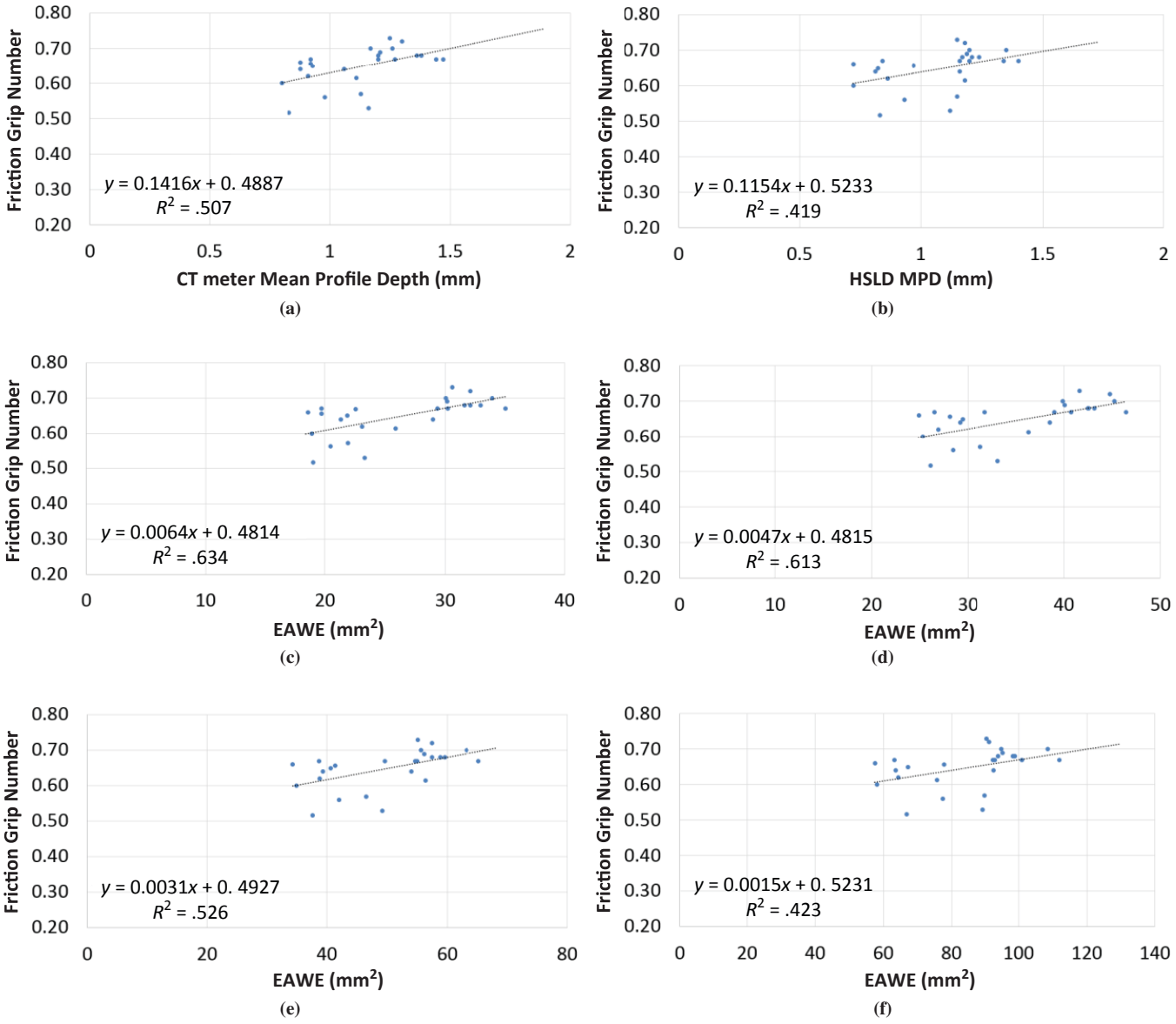

FIGURE 9 Correlations of macrotexture versus friction: (*a*) CT meter MPD versus grip number, (*b*) HSLD MPD versus grip number, (*c*) EAWE (for $d^* = 0.054$) versus grip number, (*d*) EAWE (for $d^* = 0.027$) versus grip number, (*e*) EAWE (for $d^* = 0.010$) versus grip number, and (*f*) EAWE (for $d^* = 0.001$) versus grip number.

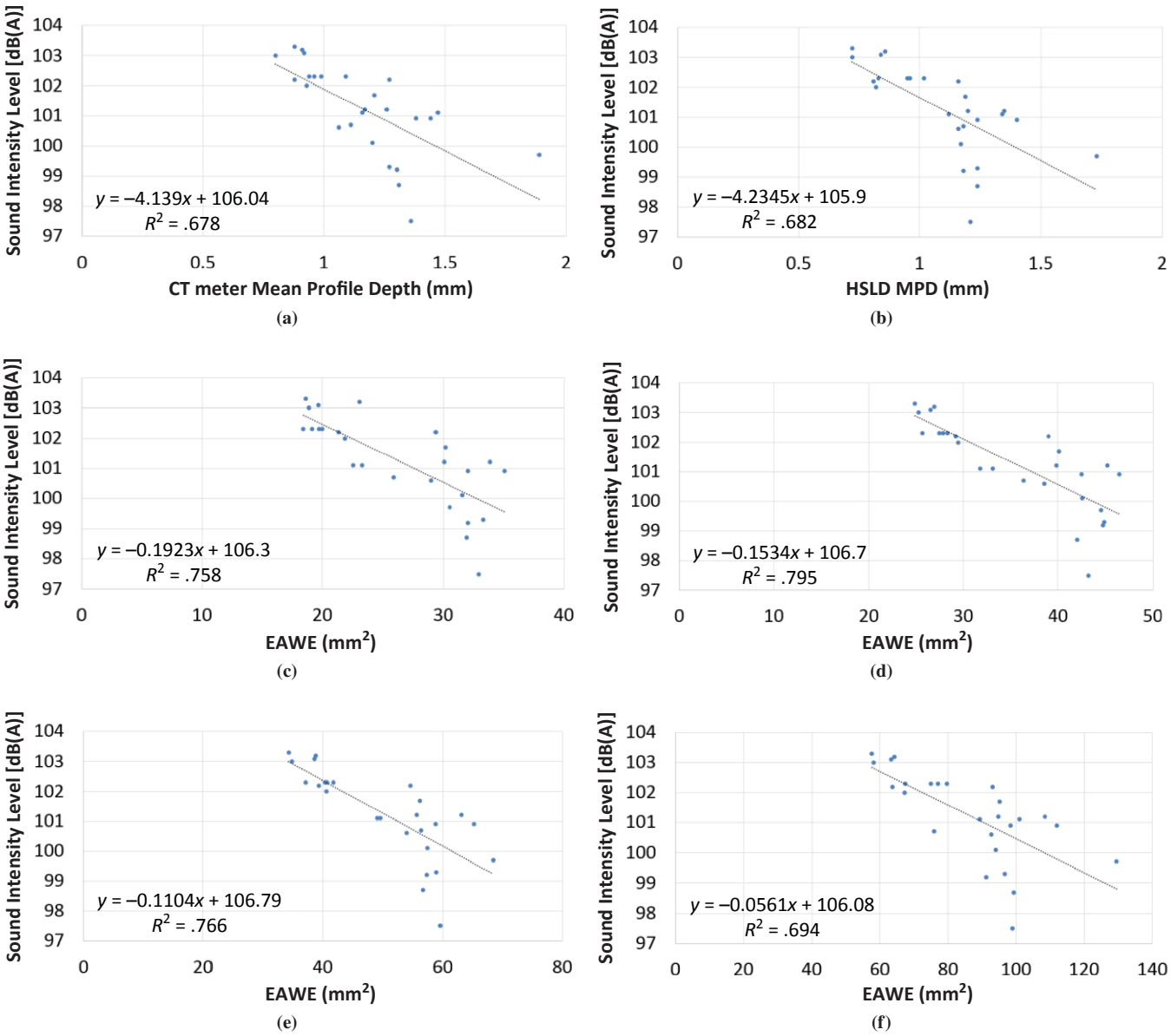

FIGURE 10 Correlations of macrotexture versus noise: (*a*) CT meter MPD versus OBSI (intensity level), (*b*) HSLD MPD versus OBSI (intensity level), (*c*) EAWE (for $d^* = 0.054$) versus OBSI (intensity level), (*d*) EAWE (for $d^* = 0.027$) versus OBSI (intensity level), (*e*) EAWE (for $d^* = 0.010$) versus OBSI (intensity level), and (*f*) EAWE (for $d^* = 0.001$) versus OBSI (intensity level).

TABLE 2 Correlation Coefficients for All Comparisons

Index	Friction	Noise
MPD (mm)		
CT meter	0.507	0.678
HSLD	0.419	0.682
EDWE (mm)		
$d^* = 0.054$	0.634	0.758
$d^* = 0.027$	0.613	0.795
$d^* = 0.01$	0.526	0.766
$d^* = 0.001$	0.423	0.694

more realistic representation of texture, correlates better with these pavement characteristics than does the MPD.

The corresponding correlation coefficients were calculated and are summarized in Table 2. Besides the reasonable improvement in correlations with friction and noise, when the EAWE (at any tire stiffness) is used instead of the MPD (CT meter MPD or HSLD MPD), it is also apparent that the EAWE correlations tend to decrease as tire stiffness increases. Both correlations, the EAWE versus friction and the EAWE versus noise, get worse and become comparable to the corresponding MPD correlations only in the case of significantly high values for tire stiffness (e.g., $d^* = 0.001$). This finding confirms that characterizing macrotexture in the "peaks" range (as MPD does by definition) is not the most appropriate approach.

DISCUSSION OF RESULTS

A high proportion of the sections with high macrotexture are open-graded asphalt mixes. These surfaces achieve high macrotexture with "negative" features and interconnected voids, which absorb some of the noise generated at the tire–pavement interface. Properties of the data set, therefore, create a confounding effect that likely leads to the strong positive correlation between macrotexture and noise. Macrotexture created by strong "positive" features (e.g., chip seals) would be expected to correlate in an opposite fashion with noise.

The implied overestimation by the MPD of a pavement's ability to drain water can be explained by the following: by definition, MPD is an index that is heavily weighted by two data points in every 100-mm base length (the highest peak for each 50-mm half–base length). The way the MPD is calculated is, then, roughly equivalent to two stages of a rigid and flat tire that only makes contact in the two highest peaks; therefore, the corresponding predicted area (voids between the tire and the pavement) is too large. On the other hand, the EAWE takes into account all data points (not just the two peaks every 100 mm) along the whole section. It also predicts better than the MPD the deformation of the tire rubber over the pavement profile and leads to a better estimation of the actual area between the tire and the pavement that is available to drain water. The MPD is a more simplistic model than the EAWE, but the latter is closer to what really happens at the tire–pavement contact. Consequently, the use of the proposed EAWE index is recommended.

SUMMARY AND CONCLUSIONS

The research described in this paper can be summarized as follows:

- This study proposed a robust three-step methodology to compute a novel index for characterizing macrotexture.
- Comparisons of current (MPD) and proposed (EAWE) macrotexture characterization indexes were performed.
- Correlations for MPD and EAWE indexes with the main pavement surface characteristics influenced by macrotexture wavelength were established for a significant variety of surface types and macrotexture levels.

The following conclusions can be drawn from the results:

- The EAWE index for characterizing pavement macrotexture appears to be a significant improvement over the MPD.
- A comprehensive comparison between the MPD and the EAWE (with different tire configurations) involving a significant number of different asphalt sections confirms that the MPD effectively overestimates the ability of the pavement to drain water under a real tire.
- The macrotexture values computed by using the EAWE (for all tire stiffnesses tested) instead of the MPD (calculated by using either the CT meter or HSLD) correlate better with friction and noise measurements.
- The use of a continuous HSLD to measure texture, and the consequent possibility of presenting macrotexture data for every location along the analyzed section (e.g., $\widehat{\text{EAWE}}$, $\text{EA}\widehat{\text{WE}}_{100}$, $\widehat{\text{EDWE}}$, or $\text{ED}\widehat{\text{WE}}_{100}$), also represents a significant improvement for macrotexture characterization. This feature may represent an important step toward more useful macrotexture characterization, not just at the project level but also at the network level.

RECOMMENDATIONS

The positive (but improved) correlation between macrotexture and noise is expected to be a function of the surface types that were included in this study. Future work should include more positively textured, nonporous materials to understand (and to characterize) better not just how much water drains under real tires but in what way.

REFERENCES

1. *Characterization of Pavement Texture by Use of Surface Profiles.* ISO, Geneva, 2009. https://www.iso.org/obp/ui/#iso:std:iso:13473:-5:ed-1:v1:en. Accessed Jan. 21, 2015.
2. Rasmussen, R. O. Pavement Texture Fundamentals. *CE News,* Vol. 25, No. 7, 2013, pp. 48–50.
3. Loprencipe, G., and G. Cantisani. *Unified Analysis of Road Pavement Profiles for Evaluation of Surface Characteristics.* Canadian Center of Science and Education, Toronto, Ontario, 2013.
4. Katicha, S. W., D. E. Mogrovejo, G. W. Flintsch, and E. de León Izeppi. Adaptive Spike Removal Method for High Speed Pavement Macrotexture Measurements by Controlling the False Discovery Rate. In *Transportation Research Record: Journal of the Transportation Research Board, No. 2525,* Transportation Research Board, Washington, D.C., 2015, pp. 100–110.
5. Katicha, S., D. Mogrovejo, G. Flintsch, and E. de León Izeppi. Latest Development in the Processing of Pavement Macrotexture Measurements of High Speed Laser Devices. Presented at 9th International Conference on Managing Pavement Assets, Washington, D.C., 2015.

6. McGhee, K. K., and G. W. Flintsch. *High-Speed Texture Measurement of Pavements.* Virginia Transportation Research Council, Charlottesville, 2003.
7. Goubert, L. *Road Surface Texture and Traffic Noise.* Presented at Norwegian Public Roads Administration Workshop: Texture and Road Traffic Noise, Oslo, 2007.
8. Klein, P., and J. F. Hamet. *Road Texture and Rolling Noise: An Envelopment Procedure for Tire-Road Contact.* Institut National de Recherche sur les Transports et leur Sécurité (INRETS), Bron, France, 2004. https://hal.inria.fr/file/index/docid/546120/filename/lte0427.pdf.
9. Sandberg, U., A. Bergiers, J. Ejsmont, L. Goubert, R. Karlsson, and M. Zoller. *Road Surface Influence and Tyre/Road Rolling Resistance.* Report MIRIAM_SP1_04. Models for Rolling Resistance in Road Infrastructure Asset Management Systems (MIRIAM), 2011. http://miriam-co2.net/Publications/MIRIAM_SP1_Road-Surf-Infl_Report%20111231.pdf.
10. von Meier, A., G. van Blokland, and G. Descornet. The Influence of Texture and Sound Absorption on the Noise of Porous Road Surfaces. In *Second International Symposium on Road Surface Characteristics,* Berlin, 1992, pp. 7–19.
11. Virginia Smart Road. Virginia Tech Transportation Institute. http://www.vtti.vt.edu/facilities/virginia-smart-road.html. Accessed July 7, 2014.
12. Mogrovejo, D. E., G. W. Flintsch, E. de León Izeppi, K. K. McGhee, and R. Burdisso. Short-Term Effect of Pavement Surface Aging on Tire–Pavement Noise Measured with On-Board Sound Intensity Methodology. In *Transportation Research Record: Journal of the Transportation Research Board, No. 2403,* Transportation Research Board of the National Academies, Washington, D.C., 2014, pp. 17–27.
13. LMI Technologies. *User's Manual: Selcom Optocator.* Sweden: LMI Technologies Inc., 2013.
14. Mogrovejo, D. E., G. W. Flintsch, E. de León Izeppi, and K. K. McGhee. Effect of Air Temperature, Vehicle Speed, and Pavement Surface Aging on Tire/Pavement Noise Measured with On-Board Sound Intensity Methodology. *IRF Examiner: Pavement Design,* Vol. 4, 2012, pp. 34–39. https://www.irfnews.org/ebooks/IRF-Examiner-14Vol4.pdf#page=34.
15. Goubert, L., and A. Bergiers. About the Reproducibility of Texture Profiles and the Problem of Spikes. Presented at 7th Symposium on Pavement Surface Characteristics: SURF 2012, Norfolk, Va., 2012. https://vtechworks.lib.vt.edu/bitstream/handle/10919/50467/SURF2012_0079.pdf?sequence=1.

The Standing Committee on Surface Properties–Vehicle Interaction peer-reviewed this paper.